Peptide Amphiphiles and their use in Supramolecular Chemistry
Versluis, F.

Citation

Cover Page

The handle http://hdl.handle.net/1887/22801 holds various files of this Leiden University dissertation

Author: Versluis, Frank
Title: Peptide amphiphiles and their use in supramolecular chemistry
Issue Date: 2013-12-09

Power struggles in peptide-amphiphile nanostructures

Inspired by the ubiquitous functions fulfilled by native proteins, the self-assembly of peptide amphiphiles (PAs) holds much promise for the creation of functional nanostructures. Typically, PAs are constructed by conjugating blocks of very different character: a hydrophilic peptide segment with a hydrophobic element (an alkyl chain, lipid, polymer or polypeptide). The resulting amphiphilicity governs the self-assembly process in aqueous solutions. This self-assembly process is guided by attractive forces (for example hydrophobic interactions, hydrogen bonding, electrostatic attraction) and repulsive forces (for example electrostatic repulsion, mechanical forces). The balance between these forces is responsible for the secondary structure of the peptide segment, and furthermore the size and shape of the assemblies that are formed. A result of PA self-assembly is that the properties of the peptide segment can be altered, as it is a general observation that peptides are more likely to exhibit a well-defined secondary structure at an interface (e.g. the corona of a micelle) than they are in solution. This characteristic of peptides can be exploited to give nanostructures with well-defined properties. The art of controlled PA self-assembly consists of carefully combining all the inter- and intramolecular forces to arrive at a material, which is both structurally well-defined and has an emergent function. In this chapter the forces that act within PA nanostructures are discussed; the effect of the hydrophobic block and peptide secondary structure on each other and on the aggregate as a whole. At the end of the review, a short section is devoted to applications of these PA nanostructures.

1. Introduction

Self-assembly is the most feasible technique for generating structures in the size range between the molecular length scale and micro fabricated structures. Moreover, using self-assembly it is possible to generate structures that are ordered at the nanometer level. Moreover, their internal order is dictated by the balance of the attractive and repulsive forces amongst molecules by which they are composed of. This balance of competing forces is determined by the design of the molecular building blocks and the supramolecular synthesis route. If the self-assembly of a system is well understood, it allows the placement of individual molecules in three dimensions with high precision. The structures can be regulated with regards to the morphology, size, and surface chemistry. Clearly this structural control is invaluable for designing interactions of the self-assembled structures with their environment. Hence, self-assembly is a very promising technique for producing functional materials whose properties can be can be designed and customized for a range of specific applications. The most comprehensive demonstration of the non-covalent assembly of functional nanostructures is found in nature. The complexity of a living organism arises from the hierarchical self-assembly of its biomolecular components, and the interactions between them. Furthermore, life cannot exist without being adaptable to stimuli. Taking proteins as an example, the amino acid sequence determines the folding of the linear polymer chain into different motifs, which are themselves folded together, resulting in proteins with precise morphology, size, and functionality. It is due to this physical and chemical precision that further levels of interactions become energetically favorable and ensue in cellular processes. Such examples include: the insertion of proteins into lipid membranes, allowing transport between lipid containers; protein binding to DNA, causing genetic information to be processed; protein-protein interactions creating supportive structures; protein binding to small molecules such as the heme complex, allowing hemoglobin to transport oxygen around the body to name but a few of the thousands of interactions and resulting life processes. The self-assembly of individual biomolecular components such as lipids, DNA, and protein folding motifs has been studied extensively. The self-assembling properties of these molecules are now understood well enough that scientists can design simple lipid-, DNA-, or peptide-based nanostructures. Of the different biomolecular components, proteins have the largest number of distinct interactions, internally and with other molecules, and hence form the greatest variety of functional

nanostructures. Unlike other biomolecular components, proteins combine diversity of structure with intricate, precise, and diverse patterns of surface chemistry. It is because of this that peptides are of particular interest for the generation of functional nanostructures using standard organic synthesis procedures. While small peptide motifs can be designed to self-assemble into well-defined architectures, the self-assembly of entire synthetic proteins, consisting of multiple motifs, is less developed. Synthetic proteins are potentially extremely useful, but the intra- and intermolecular interactions must be well managed and currently this is not readily achieved. The combination of multiple protein motifs, each contributing structural and functional features, becomes unwieldy. It is more practical to combine peptide sequences with a synthetic component/s that provides either structure or function. For the generation of self-assembled nanostructures, peptide amphiphiles are commonly employed. Peptide amphiphiles (PAs) commonly consist of peptides that can confer both structural and functional elements depending on their location within the sequence and a hydrophobic non-peptidic element to drive assembly in water. The hydrophobic unit is often a lipid or alkyl chain, or less commonly, a polymer or polypeptide.[1] The coupling of a peptide to a hydrophobic unit yields an amphiphile and is a relatively simple way of inducing supramolecular structure in aqueous solution. In general, the hydrophobic element induces aggregation of the PA in aqueous solution, while the hydrophilic peptide block displays an ordered pattern of chemical functionality at the interface of the self-assembled structure and the aqueous solution and therefore interacts with molecules in the environment. However, as with the molecular components of a cell, or the different motifs in a protein, the different sections of a PA cannot function independently of one another, they each modify the structure of the other. The balance of many small forces determines the overall morphology, size, and functionality of the structures, and a deeper understanding of these factors is important for guiding future research, and for customizing PAs for specific applications. This chapter summarizes the molecular perturbations that arise from conjugating such disparate blocks together—the power struggles within PA nanostructures. Here, only PA's which consist of a hydrophilic oligopeptide domain coupled to one or more alkyl or lipid tails are considered. First, the effects that the hydrophobic unit can have on the structure of the peptide block is examined, then various other ways in which peptide secondary structure can be manipulated are

discussed, which feeds back to the structure of the hydrophobic block, and of the aggregate as a whole.

2. Effects of the hydrophobic block on the peptide block

2.1 Induction and stabilization of peptide interactions

Whereas short peptides are typically unstructured, when they are conjugated to hydrophobic tails they often adopt a well-defined secondary structure upon their hierarchical self-assembly. To understand this phenomenon, two effects which contribute significantly to stabilizing the 3-dimensional structure of a peptide need to be taken into account. Firstly, peptide chain length. Generally, more repeats of a structure inducing peptide sequence increases the stability of the secondary structure as increasing the number of non-covalent interactions yields more stable assemblies. Secondly, the local peptide concentration. Higher peptide concentrations yield more stable secondary structures. The local concentration can be raised, for example, by covalently linking the peptide chains or by coupling a hydrophobic moiety to the peptide. In the latter case, aggregation of the peptide amphiphile brings the peptide segments into close proximity, thereby increasing the effective concentration. In this process, the peptide reorients itself in order to accommodate *intra* and *inter*molecular non-covalent bonds. Hence, conjugating a hydrophobic block to a peptide can induce and stabilize its secondary structure within the assembly. A consequence of this phenomenon is that peptides often show a different behavior when they are in solution compared to when they are attached to the surface of a self-assembled structure. One of the earliest systematic enquiries on the stabilization of peptide secondary structure by conjugation with alkyl tails was conducted by Yu et al.,[2] who studied peptide-amphiphiles with a collagen-model head group, (Gly-Pro-Hyp)$_4$-[IV-H$_1$]-(Gly-Pro-Hyp)$_4$. IV-H$_1$ is a type IV collagen derived sequence, which is known to promote melanoma cell adhesion and spreading and it does not form triple helices on its own. The Gly-Pro-Hyp sequence is known to form collagen-like triple helices. The incorporation of a C6 tail was sufficient to double the α-helicity of the peptide, and to stabilize the triple-helical structures, causing an increase in the melting temperature from 35.6 ℃ to 42.2 ℃, as was shown by circular dichroism (CD) data. Upon increasing the length of the hydrocarbon chain the T$_m$ subsequently increased by about 2.7 ℃ per carbon atom. The introduction of the alkyl tail induced a higher level of 3D organization of the peptide segment and stabilized it. Peptide segments with a

well-defined secondary structure can increase the biological relevance of PA nanostructures. An example of this principle was demonstrated by Chu-Kung et al.,[3] who investigated the structural and antimicrobial properties of a peptide, SC4 (Lys-Leu-Phe-Lys-Arg-His-Leu-Lys-Trp-Lys-Ile-Ile), and the corresponding PA C_{12}–SC_4, in which the peptide is conjugated to a twelve carbon atom fatty acid. Many antimicrobial peptides have in common that they are able to form a three-dimensional structure with a distinct hydrophobic and hydrophilic face. Furthermore, a hydrophobic segment is desirable, to aid membrane insertion, yielding a more effective compound. Additionally, fatty acid conjugation can induce well-defined peptide secondary structures at low concentrations, which is highly desirable with respect to host toxicity. The minimum bactericidal concentration, which is the minimum concentration at which 99.9% of bacteria are killed, was found to be 15 fold lower for C_{12}–SC_4 than for SC_4. To investigate the secondary structure under conditions similar to a cellular environment, SC_4 and C_{12}–SC_4 were added to lipid vesicles. Circular dichroism results showed that SC_4 has 27% α-helical structure, compared to 100% for C_{12}–SC_4. The peptide folding, in turn, leads to a 3D peptide structure with a clear hydrophobic as well as a hydrophilic face. The increased antimicrobial activity for C_{12}–SC_4 compared to SC_4 is most likely a combination of two factors: (1) a high percentage of α-helicity for C_{12}–SC_4, which leads to a peptide with two distinct faces and (2) insertion into the membrane due to the alkyl tail, which ensures the correct location of the PA. Typically, PAs contain a hydrophobic block at one end of the peptide, usually at the N-terminus. Löwik et al.[4] designed a PA in which the peptide was intended to fold into a β-turn, using a sequence derived from a protein of a malaria parasite. The goal was to stabilize this β-turn sequence at the surface of liposomes, as this motif is present in many native molecular recognition events. When the peptide was only alkylated at the N-terminus and the resulting PA inserted into liposomes, an unordered secondary structure was observed. However, when both termini of the peptide were alkylated, and the PA added to a dispersion of liposomes, a well-defined β-turn structure was observed. In this case, both hydrophobic tails can dock into the liposome membrane, causing the peptide to fold, mimicking the β-turn motif found in proteins. This result shows that multiple hydrophobic blocks can be required to obtain the desired secondary structure. Moreover, conformational restriction of biologically active sequences, like RGD, can provide enhancement of the binding affinity for a specific receptor, thereby increasing

receptor selectivity.[5] Furthermore, the degradation of peptides by enzymes (i.e. proteases) can be significantly reduced by stereochemical or conformational restriction.[6] Previously, it was observed that incorporation of a hydrophobic tail can induce secondary structure formation, however, it is not always sufficient. Sometimes, a second structure-inducing moiety is needed. Malkar et al.[7] opted to use the SPARC$_{119-122}$ sequence (Lys-His-Gly-Lys), which is known to stimulate endothelial cell proliferation and angiogenesis when it has a helical conformation. However, this peptide by itself does not form a defined 3D structure. Therefore, to improve the activity and prevent degradation, it was conjugated to a model α-helical sequence: Lys-Ala-(Glu-Ile-Glu-Ala-Leu-Lys-Ala)$_2$, abbreviated as 16r. A set of PAs was subsequently synthesized by modifying the peptide at the N-terminus with an alkyl chain ranging from 6 to 18 carbon atoms. The resulting PAs consist of three regions, which all have their specific characteristics and function: a hydrophobic anchor (1), which stabilizes the secondary structure of a peptide segment (2), which naturally has the tendency to form an α-helical secondary structure, and induces the ordered secondary structure for the biologically relevant peptide segment (3). With these PAs, well-defined secondary structures could be obtained and their surface bioactivity was studied. The SPARC119–122 segment was not α-helical (whether or not it was alkylated) and when it was conjugated to the 16r sequence; 30% α-helicity was observed. However, when 16r-Tyr-SPARC119–122 was alkylated the α-helical content of the PAs increased significantly with increasing alkyl chain length, from 51% for C6 to 96% for C18. From these results, it is clear that for SPARC119–122 to adopt a well-defined secondary structure, two structural elements are required, the hydrophobic tail and the α-helix forming peptide. The incorporation of a double bond in the C18 tail makes the tail more flexible, thereby decreasing the hydrophobic interactions, which led to a decrease in the α-helicity of the peptide segment from 96% to 47% and lower thermal stability. The addition of a hydroxy group at the C-12 position of the unsaturated C18 chain led to intermolecular hydrogen bonding, and a more rigid PA tail, accompanied by an increase of α-helicity of the peptide from 47% to 62%.

2.2 Moderation of peptide interactions.

Typically, β-sheet forming peptides are comprised of alternating hydrophobic/hydrophilic amino acid residues.[8] When β-sheet forming peptides

aggregate in aqueous solution, they tend to form rigid amphiphilic assemblies. Due to the strong interpeptidic interactions, stimuli-unresponsive aggregates are formed. In the previous section, the hydrophobic blocks of PAs were shown to promote and stabilize peptide secondary structure in PA assemblies. In this section, the hydrophobic tails have a different effect on the peptide: they moderate interpeptide interactions, enabling the controlled aggregation of β-sheet forming PAs. Peptides can form stable monolayers at the air–water interface and display a well-defined secondary structure. However, directed self-assembly to create two-dimensional (2D) order in the monolayer is not readily achieved by peptides which solely consist of β-sheet forming amino acids, as they tend to form structures with only one-dimensional (1D) order. A 2D monolayer consisting of PAs was investigated by Matmour et al.,[9] who studied the self-assembly behavior of a p-conjugated oligomer-peptide conjugate. An oligo(p-phenylenevinylene) trimer (OPV) was functionalized with a pentapeptide (Gly-Ala-Gly-Ala-Gly) which has been identified as an important repeat sequence in crystalline β-sheet domains yielding OPV-1. A monolayer of OPV-1 was formed at the liquid-solid interface, with highly oriented pyrolitic graphite as the solid support and 1-octanoic acid as the liquid phase, and characterized by scanning tunneling microscopy (STM) and infrared (IR) spectroscopy. OPV-1 monolayers revealed the formation of antiparallel β-sheet conformation **(Figure 1)**. This result shows that the packing of the PA at the solid-liquid interface is a result of the interplay between peptide interactions and hydrophobic interactions. However, it is important to note with these kinds of studies that the highly ordered surface of mica or HOPG can impose structure upon the monolayers themselves which would otherwise be not present. The peptide segment has the natural tendency to form β-sheet domains, whereas the OPV part of the PA influences the structure by enhancing the hydrogen bonding efficiency between the peptide strands as well as by acting as a β-sheet breaker, a feature which is similar to proline residues.[10]
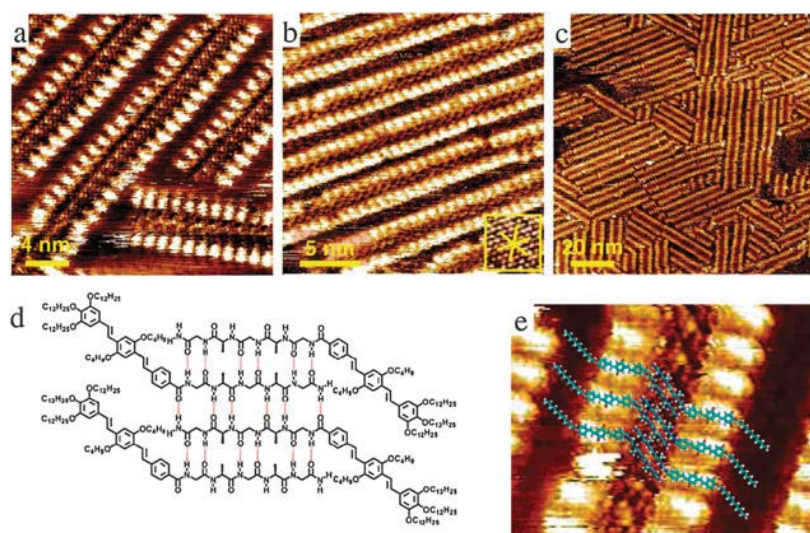
Figure 1. *(a)–(c) STM images of the OPV-1 monolayer, which show that the molecules are stacked antiparallel (bright areas correspond to OPV, dark areas to the peptide). (d) Molecular model of the antiparallel β-sheet conformation, (e) superimposed on an STM image. Adapted from ref. 9.*

β-sheet breakers are placed at the peptide termini and induce two-dimensional registry of the assembled peptides rather than one-dimensional ordering. While the hydrophobic block of a PA induces its aggregation and stabilizes the secondary structure of the peptide segment, it can also allow for adaptability of the assemblies, whereas the corresponding peptidic assembly is too rigid to respond to changing conditions. In a contribution by Cavalli et al., the water-soluble motif (Leu-Glu)$_4$ was modified at the N-terminus with a phospholipid tail. As it consists of alternating hydrophobic/hydrophilic amino acid residues this molecule has a tendency to form β-sheet secondary structures and well-defined monolayers at the air–water interface, in which the lipids were folded on top of the peptide residues, acting as a hydrophobic anchor for the peptides.[11] The second function of the lipid tail is to act as a β-sheet breaker, which, as mentioned previously, can be used to promote 2D structures. Both the peptide by itself, as well as the peptide component of the PA were found to be in an anti-parallel β-sheet conformation at the air–water interface, which gave rise to an array of well-ordered carboxylic acid groups oriented towards the aqueous phase. When the PA was compared with the peptide alone during surface pressure-molecular area isotherm experiments, it was observed that upon compression the PA goes through a much larger range of area per molecule, demonstrating the increased adaptability of the PA compared to the peptide. Subsequently, these monolayers were

investigated as well-defined two-dimensional templates for the mineralization of $CaCO_3$.[12] It was found that under the monolayer consisting of the lipopeptide, mainly indented crystals appeared, which were largely suppressed under the monolayer of the unmodified peptide. It was proposed that this difference was due to the fact that the peptide alone is less able to reorient itself due to the rigidity of the β-sheet. The conjugation of this peptide motif with a phospholipid leads to a more stable and more adaptable assembly. While conjugating a hydrophobic block to a peptide can induce secondary structure formation, attaching a hydrophilic block can prevent that process from taking place. In the following example, both a hydrophobic and a hydrophilic segment were coupled to a peptide. Meijer and co-workers[13] introduced a hydrophilic PEG moiety (MW ~3000 g/mol) at the C-terminus of a hexapeptide Lys-Thr-Val-Ile-Ile-Glu (KTVIIE), which naturally forms fibrils. CD spectra and transmission electron microscopy (TEM) images indicated that for KTVIIE-PEG, β-sheet formation and concomitant fiber formation did not take place, as PEG has the tendency to wrap around peptides.[14] However, when a hydrophobic chain was conjugated (via a UV-sensitive nitrobenzyl linker) to the N-terminus of the peptide KTVIIE-PEG, β-sheet formation as well as fiber formation was observed. Upon irradiation, the linker was cleaved, and resulted in the detachment of the alkyl tail. Consequently, the peptide returned to the dissolved state, and adopted a random coil secondary structure. Thus, by introducing both segments where one is cleavable, control is achieved over secondary structure and the resultant aggregate morphology. As the PA assemblies contain distinct hydrophilic and hydrophobic regions, it is possible to locally incorporate guest molecules, which can alter the properties of the PA nanostructures. Paramonov et al.[15] investigated the physicochemical properties of an acylated β-sheet forming oligopeptide **(Figure 2a)** both with and without additional lipids. Cryo-TEM and CD data indicate that upon dispersing the PA in aqueous solution, nanofibers are formed **(Figure 2b** and **c)** with a hydrophobic core and a peptide exterior, with the peptide adopting a β-sheet secondary structure. Hydrophobic interactions, due to the alkyl tail, govern the self-assembly of these amphiphilic peptides into nanofibers which are further stabilized by the folding of the peptide region into a β-sheet secondary structure, which is due to hydrogen bonding.
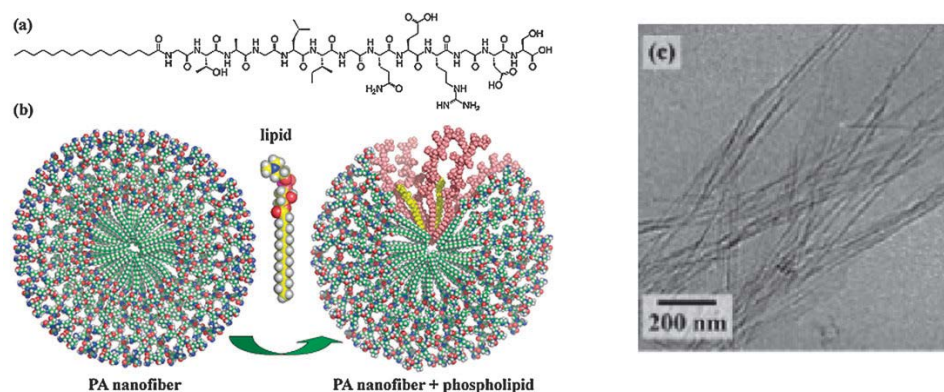
Figure 2. *(a) Molecular structure of the PA. (b) Molecular model of the self-assembled PA nanofiber. The added phospholipids are incorporated in the fiber. (c) Cryo-TEM image of the nanofibers. Adapted from ref. 15.*

The nanofibers form a network, giving rise to hydrogel formation. By introducing phospholipids into the amphiphilic peptide nanofibers, the mechanical properties of the resulting hydrogel as well as the peptide secondary structure were altered. These two parameters showed a strong correlation: both the mean molar ellipticity per amino acid residue in circular dichroism as well as the storage modulus in oscillatory rheology measurements showed a maximum when 5 mol% of lipids was incorporated, and a sharp decrease when higher or lower amounts were used. This indicates that the interactions between lipids and PA molecules induce a change in the molecular structure of the nanofibers, which directly influences the macroscopic properties.

2.3 Prevention of peptide interactions

To obtain PA nanostructures with a well-defined 3D conformation of the peptide segment, a balance needs to be found between the forces acting within the PA assembly. For example, when the hydrophobic forces dominate, uncontrolled aggregation can occur in which the peptide is too sterically hindered to adopt a well-defined secondary structure. Behanna et al.[16] investigated a group of four peptide amphiphiles consisting of two peptides that were positively charged (**1, 3**) and two that were negatively charged (**2, 4**) (**Figure 3**).
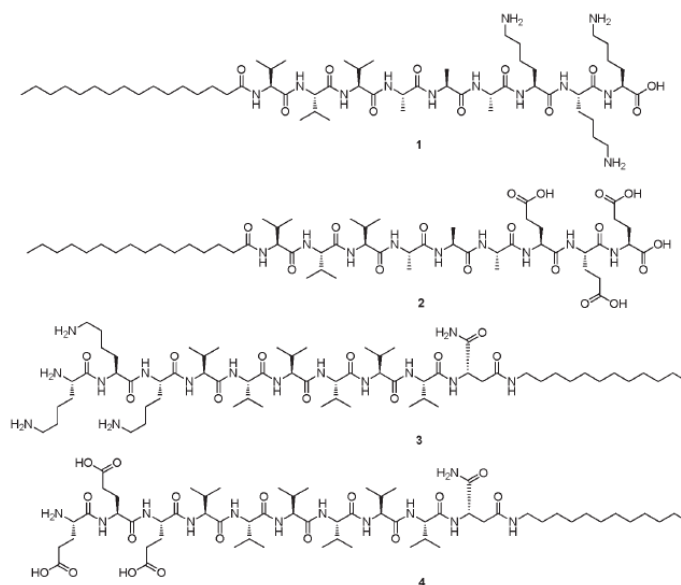
Figure 3. *Scheme of the four charged PAs used to make nanofibers. PAs 1 and 3 are positively charged and PAs 2 and 4 are negatively charged. Palmitic acid is coupled to the N-terminus for PAs 1 and 2 whereas dodecylamine was coupled to the C-terminus of 3 and 4. Adapted from ref. 16.*

In these PAs palmitic acid is either coupled to the C-terminus (1, 2) or to the N-terminus (3, 4). When individual PAs were dispersed in aqueous solution, nanofibers were formed but only molecule 1 exhibited a β-sheet signature, for peptides 2–4 random coils were observed. However, annealing of samples 2–4 caused a transition from a random coil to a β-sheet conformation. This observation was attributed to the disassembly of the fibers, with the resulting CD signal being derived from individual PA molecules in solution. The reversibility of this process renders it likely that the fibers are in a thermodynamically stable state. It further shows that aggregation of peptides 2–4, which is driven by hydrophobic interactions and causes steric hindrance between the peptide segments, prevented β-sheet formation. Furthermore, when the peptide–peptide interactions were increased by reducing the electrostatic interactions (adding salt, adjusting pH), nanofibers in which the peptide segment exhibited a β-sheet conformation were observed for all the individual PAs. This shows that β-sheet formation within the nanofibers can only occur when the correct balance is achieved between peptide–peptide interactions and hydrophobic interactions. Ayres et al.[17] investigated a peptide, Ser-(Ala-Gly)$_2$-Ala-Glu-(Ala-Gly)$_2$-Ser, which was modified with large methyl methacrylate (MMA) polymer chains using atom transfer radical

polymerization (ATRP). This peptide was anticipated to form β-sheet domains due to propensity of the Ala-Gly motif to promote β-sheet structures.[18] The PA self-assembled into a mixture of polymersomes and large compound micelles (LCMs). The formation of these aggregates was caused by phase separation of the hydrophilic peptide block and the hydrophobic MMA block. However, the expected β-turn structure of the peptide part was not observed. The strong hydrophobic interactions between the MMA blocks overwhelm the intrinsic tendency of the peptides to fold into the β-sheet hairpin motif. When the overall hydrophobic force is too large, i.e., the hydrophobic interactions are stronger than hydrogen bond formation, the peptide is too sterically hindered to fold into the intended secondary structure.

2.4 Controlling aggregate type by the length of the hydrophobic block

Elgersma et al.[19] showed that the aggregation behavior of an amylin (20–29) peptide sequence can be significantly altered by alkylating the peptide with several chains, ranging from C_2 to C_{18}. To be able to incorporate these alcohols, a single β-aminoethane sulfonyl amide moiety was incorporated in the amylin peptide and the increased acidity of the sulfonyl amide NH was used for the regioselective alkylation of the peptide backbone. The different compounds were tested for gelation behavior, secondary structure formation (using FT-IR and CD), and the shape of the aggregates were monitored by TEM. The original amylin sequence forms an opaque gel, composed of amyloid fibrils and other β-sheet structures. The incorporation of the β-amino acid, prevented β-sheet formation in the peptide and a random coil secondary structure was observed. Furthermore, while native amylin forms amyloid fibrils, the modified peptide forms twisted lamellar sheets. Alkylation of the NH of the sulfonamide moiety with the shortest alcohols prevented aggregation and secondary structure formation completely. By increasing the length of the alkyl tail further, aggregation changed from peptide-driven to lipid-driven. Depending on the size of the alkyl group, different morphologies of the aggregates were observed and they all lacked a clear secondary structure in the peptidic component. This result demonstrates that the resultant aggregate can be controlled by changing the length of the alkyl tail.

3. Influence of peptide–peptide interactions on the aggregate as a whole

In the type of PAs addressed in this chapter, the headgroups are formed by hydrophilic oligopeptides, which form the corona of the self-assembled nanostructures. The well-defined secondary structures that these peptide segments display, allow for the placement of atoms to high precision at the surface of the assemblies. Whereas β-sheet forming PAs tend to pack into a cylindrical morphology, a coiled-coil forming peptide amphiphile was found to form star-like micelles, as was shown by Boato et al.[20] The coiled-coil motif consists of 2 or more α-helices, which are coiled together. The basis of these particles was an acylated coiled-coil forming peptide. In this system, both the hydrophobic interaction between the lipid tails as well as the interaction between the peptide chains to form coiled-coils drives self-assembly. Coiled-coil binding assembles the PAs into parallel trimeric helical bundles. The lipid tails, which are located at the N-terminus, drive the self-assembly of B24 coiled-coil bundles into stable micelles. The coronas of these micelles are highly structured; each 'arm' is represented by a bundle of three coiled-coil forming peptides. Furthermore, synthetic antigens were coupled to the C-terminus of the lipopeptide building block. The result is a B20 nm star-like micelle with antigens decorating the surface, which can be recognized by B-cells (lymphocytes that play a large role in the humoral immune response) **(Figure 4)**.
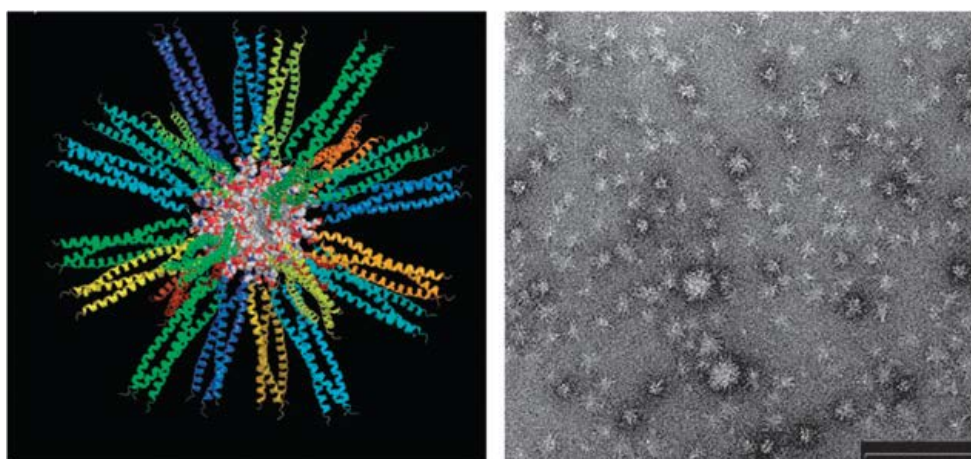

Figure 4. *(left) Computer generated image of the star-like micelle consisting of 24 helical bundles. (right) TEM image showing the morphology of the assemblies formed by the PA. Scale bar = 100 nm. Adapted from ref. 20.*

While the previously mentioned coiled-coil based PA and ordinary surfactants such as SDS tend to form spherical micelles, β-sheet forming PAs have a strong tendency to form fibers, which is due to intermolecular hydrogen bonding.[21] Fibers typically have a substructure of twisted or helical ribbons, which is due to the chiral character of natural amino acids. It was found that disruption of hydrogen bonds close to the core of the assembly (near the alkyl tail) eliminates the ability of the PA to form elongated nanofibers, emphasizing the importance of the core amino acids in structure stabilization. The amino acid residues at the outside of the helix are too distant from one another to accommodate hydrogen bonds (**Figure 5**). As compared to spherical micelles, cylindrical micelles do not exhibit curvature in two directions but only one. This is due to the restriction laid upon the assembly by the specific orientation of the peptide segments that is required to maximize hydrogen bonding in the z-direction of the fiber.
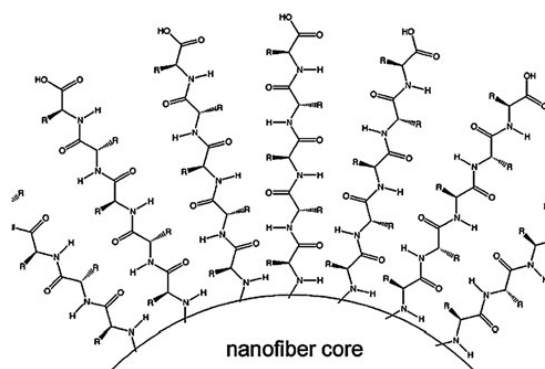

Figure 5. *Schematic drawing of part of the corona of a PA nanofiber (looking in the Z-direction). Due to the packing, core amino acids are in closer proximity then peripheral amino acids and thereby, contribute more to H-bonding.*

3.1 Changes in peptide secondary structure induce morphological changes in the assemblies

Peptide–peptide interactions can exert a large influence on the morphology of PA nanostructures. When the peptide segment of a PA organizes into a well-defined secondary structure at the surface of for example a micelle, the packing of the PA within the nanostructure can be altered, yielding an altered morphology for the assembly. The following examples show various ways in which peptide secondary structures within PA assemblies can be altered. For PA fibers, a change in the

secondary structure of the peptidic corona can trigger in a change in the assembly's superstructure. This reorganization can be triggered externally, for example by changing the pH or salt concentration, but in some cases it can also occur spontaneously. Shimada et al.[22] studied the self-assembly properties of a peptide amphiphile in which an α-helical peptide is coupled to a C_{16} tail. Above the critical micelle concentration (cmc), this PA forms spherical micelles in solution with the corona formed by the peptide moiety, which adopts a partly α-helical and partly random coil conformation. Upon aging for 13 days however, the secondary structure changed to a β-sheet conformation and the morphology concomitantly changed from spherical to wormlike micelles. The spherical micelles are kinetically favored whereas the cylindrical micelles are thermodynamically more stable. The process is faster when the temperature is raised, from 13 days at 25 ℃ to 100 min at 50 ℃. The authors hypothesize that the β-sheet formation reduces the effective area per head group (i.e. per peptide), leading to less complete coverage of the hydrophobic core and therefore, enhanced attraction. The morphology of the assembly as a whole and the secondary structure of the peptide amphiphile within the assembly are determined cooperatively and simultaneously. Muraoka et al.[23] showed that molecular changes adjacent to the β-sheet domain of a PA can have a large influence on the secondary structure of the peptide, and hence the morphology of the aggregates that are formed upon dispersion of the PA in an aqueous environment. In this case the molecular change is caused by irradiation. To investigate this effect two PAs were studied, both consisting of the amino acid sequence Gly-(Ala)$_2$-(Glu)$_2$-Arg-Gly-Asp-Ser, which was coupled at the N-terminus to an alkyl tail, and with RGDS functioning as a bioactive epitope. The difference between the peptides was the presence (5) or absence (6) of a photocleavable 2-nitrobenzyl at the N-terminus of the peptide segment as a side chain (**Figure 6**).
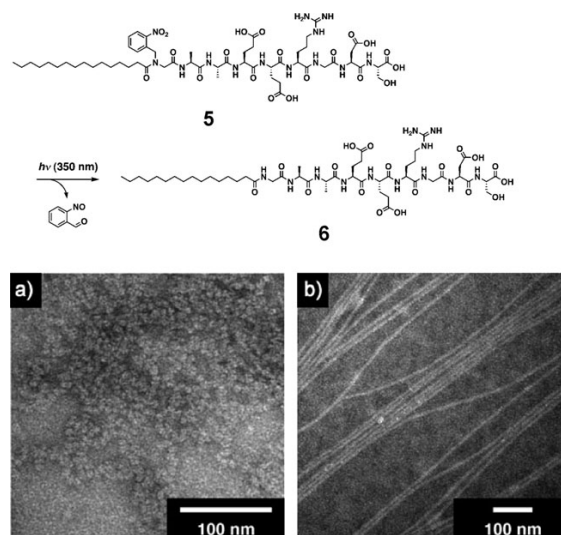
Figure 6. *(Top) Molecular structures of PAs 5 and 6. (Bottom) TEM images of (a) PA 5 and (b) PA 6. In compound 5 the nitrobenzyl group is present, hindering efficient β-sheet formation, resulting in spherical micelles. Upon photocleavage of the nitrobenzyl group an increase in β-sheet formation leads to a transition from spherical to cylindrical micelles. Adapted from ref. 23.*

Under self-assembling conditions, PA **5** formed a transparent solution, while **6** formed a transparent gel. TEM imaging revealed that compound **5** assembled into spherical micelles and **6** into nanofibers **(Figure 6)**. CD measurements showed a strong β-sheet signal for compound **6** and only a weak signal for **5**. Upon irradiation of the nanospheres composed of **5**, the 2-nitrobenzyl group was cleaved resulting in compound **6.** A transition in secondary structure from mainly random coil to β-sheet was observed in parallel with a transition from a spherical to a cylindrical micellar morphology. These results show that: (1) hydrogen bonding between amino acid residues close to the core of the assembly is vital for β-sheet formation and (2) the reorientation of the peptides to accommodate hydrogen bonding, which leads to β-sheet formation, results in fiber formation, with hydrogen bonding taking place in the z-direction of the PA nanofiber. In an elegant contribution, Cui et al.[24] showed that that through modification of PA concentration and pH peptide interactions various morphologies can be obtained in a PA system. An alkylated tetra peptide with alternating hydrophilic and hydrophobic amino acid residues (Val-Glu-Val-Glu) was shown to undergo strong planar growth upon dispersion in an aqueous environment, thereby losing the curvature normally observed in fibers, and forming nanobelts. This β-sheet forming PA forms flat nanobelts due to the strong interactions between the

side chains of the amino acids, which favor a flat morphology over a curved one **(Figure 7)**. When in a β-sheet conformation, the hydrophilic and hydrophobic side chains are oriented towards opposite sides of the peptide backbone. Due to hydrophobic interactions, the valine side chains display a strong affinity for one another in aqueous solution. This results in an assembly consisting of a flat morphology. Atomic force microscopy (AFM) imaging revealed that the length of these nanobelts reaches up to 0.1 mm and that the thickness (4.3 nm) corresponds to a single PA bilayer **(Figure 7)**. At low pH, when the glutamic acid side chains are protonated, multilayered aggregates also form. These structures can be separated into single bilayer assemblies by raising the pH. This can be accounted for by the deprotonation of the glutamic acid residues, which leads to electrostatic repulsion between the peptide strands. This also results in the formation of grooves between PA dimers, while the nanobelt morphology is maintained due to hydrophobic interactions between the alkyl tails and between valine side chains.
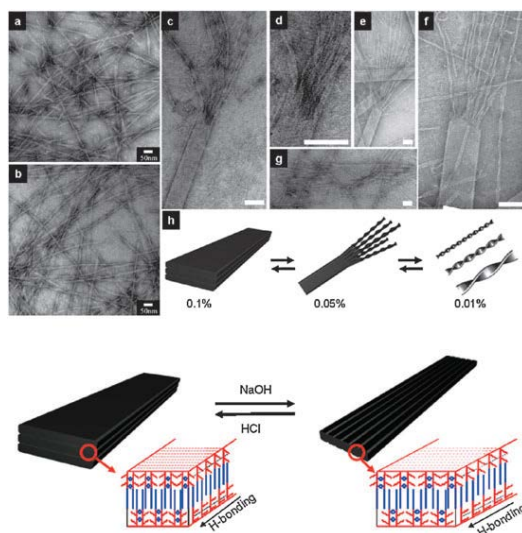

Figure 7. *(Top) TEM images of C16VEVE. (a,b) At low concentrations, mainly twisted nanoribbons are observed. (c)–(g) Nanobelts with twisted nanoribbons sprouting from one end are observed at higher concentrations. (h) Schematic representation of the change in morphology of the aggregates with varying concentrations. (Bottom) At low pH, C16VEVE forms stacks of bilayers, at high pH single bilayers with grooves are observed. Adapted from ref. 24.*

Upon dilution, the nanobelt ends show a tendency to form twisted nanoribbons, as was indicated by TEM data. At lower concentrations hydrophobic interactions between the valine side chains, which are responsible for the flat morphology of the

nanobelts, are too weak to overcome the natural tendency of β-strands to form twisted β-sheets, and as a result, the structure becomes helical. Reversible changes in the peptide secondary structure can also induce reversible changes in the self-assembled superstructures. Versluis et al.[25] constructed a hierarchical supramolecular assembly by decorating alkylated β-cyclodextrin vesicles non-covalently with adamantane-modified octapeptides (Adamantane-(Leu-Glu)$_4$) **(Figure 8)**. In this two-component system, three orthogonal interactions are combined: (1) hydrophobic interactions between alkylated cyclodextrins, resulting in vesicles; (2) the inclusion complex formation of β-cyclodextrin and adamantane, which is based on size-specific hydrophobic interactions; (3) intermolecular hydrogen bonding between adjacent peptide strands. When the peptide hybrid is added to the cyclodextrin vesicles an inclusion complex is formed where the adamantane moiety binds in the hydrophobic cyclodextrin cavity. At pH 7.4, the glutamic acid residues are largely deprotonated resulting in electrostatic repulsion, and the peptide adopts a random coil secondary structure. On the other hand, after acidification to pH 5.0 the glutamic acid side chains are partly protonated and the peptides form β-sheet domains at the surface of the vesicles. This partial protonation induces a morphological change of the system from a sphere to a fiber. Fluorescence measurements showed that the morphological change from a sphere to a fiber concomitantly induces the release of a large part of the content from the vesicular assembly. The transition of the secondary structure of the peptide, as well as the morphology of the whole complex is reversed by increasing the pH again. Furthermore, as has been shown by several examples in this review, these short peptides require an interface (i.e. the vesicle surface) combined with an optimal pH range in order to form β-sheet domains.
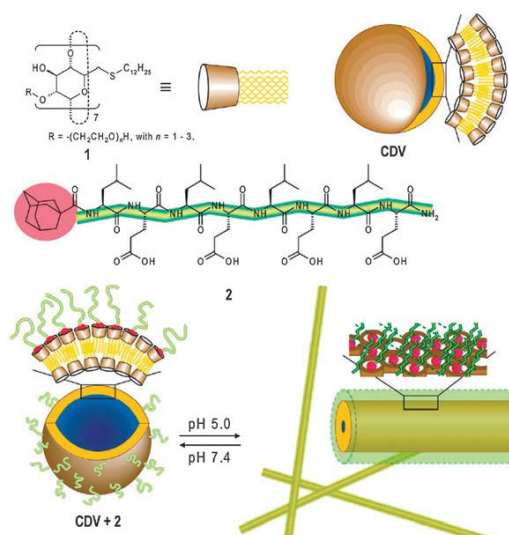
Figure 8. *(1) Molecular structure and model of the β-cyclodextrin derivative, which self-assembles into vesicles (CDV). (2) Molecular structure of Ad-(Leu-Glu)4, which forms an inclusion complex at the surface of the CDVs. When the pH is lowered from 7.4 to 5.0, a change in the secondary structure of the peptide from random coil to β-sheet is observed, together with a transition from a spherical vesicle to a tubular structure. Adapted from ref. 25.*

3.2 Molecular recognition induces morphological changes in the assemblies

Molecular recognition refers to the specific interaction of two or more molecules via non-covalent bonds, for example by hydrogen bonding, hydrophobic interactions or electrostatic interactions. Upon molecular recognition, the conformation of one or more of the participating molecules can undergo three-dimensional structural reorganization. Upon peptide reorganization in a PA, the morphology can be altered significantly. Therefore, this section is devoted to the structural reorganization of PA nanostructures, as caused by molecular recognition between different molecules. Marsden et al. designed a non-covalent triblock copolymer which was based on a coiled-coil peptide motif.[26, 27] An α-helical coiled-coil pair (denoted as E and K) was chosen to act as molecular velcro in order to connect polystyrene (PS), conjugated to the N-terminus of peptide E, with poly(ethelyne glycol), coupled to the C-terminus of peptide K.[27] These molecules self-assemble over two length scales upon dispersion in solution: the specific association of the peptide pair leads to the formation of the new amphiphilic triblock copolymer PS-E/K-PEG, which further self-assembles into rodlike micelles. Increasing the temperature reduced the coiled-coil molecular recognition results in dissociation of the K-PEG component from the rodlike micelles,

and the structural conversion of the PS-E amphiphile to spherical micelles. Short amino acid sequences are able to interact with biological entities such as cells and DNA. These epitopes can easily be incorporated into PAs, and when the nanostructure is formed the biologically active sequences are located on the outside of the assembly, making them available to interact with the biological target. Furthermore, upon binding the morphology of the assembly can change significantly as is illustrated by an example from Bitton et al.,[28] who examined the self-assembly properties of a DNA-binding amphiphilic peptide. This PA consists of three parts: the head group composed of a DNA binding sequence, a spacer based on a coiled-coil nucleating septet, and a hydrophobic tail of monoalkyl methacrylic acid. In aqueous solution this peptide forms a tubular structure (bilayer or multilayer membranes of an amphiphilic molecule wrapped in a cylinder), as was confirmed by cryo-TEM and small angle X-ray scattering. The peptide headgroup is partly α-helical, partly random coil. Subsequently, calf thymus (ct) DNA was added and induced further folding of the peptide headgroup into a 100% helical conformation. Small angle neutron scattering (SANS) data suggests that the addition of DNA also significantly changed the aggregate geometry to a membrane like lamellar structure. This example shows that molecular recognition can lead to significant changes in the morphology of the PA assembly. Again using molecular recognition, the next example further demonstrates the potential of this approach. Here, complementary peptides incorporated into individual liposomes undergo specific coiled-coil binding, leading to their fusion. The inspiration for this research was derived from nature, where three complementary SNARE proteins (SNARE = soluble N-ethylmalemeide-sensitive factor attachment protein receptor) mediate membrane fusion by the specific formation of a coiled coil complex that bridges membranes.[29] A synthetic reduced SNARE model to mediate the fusion of liposomes was designed by Marsden et al. (**Figure 9**).[30]
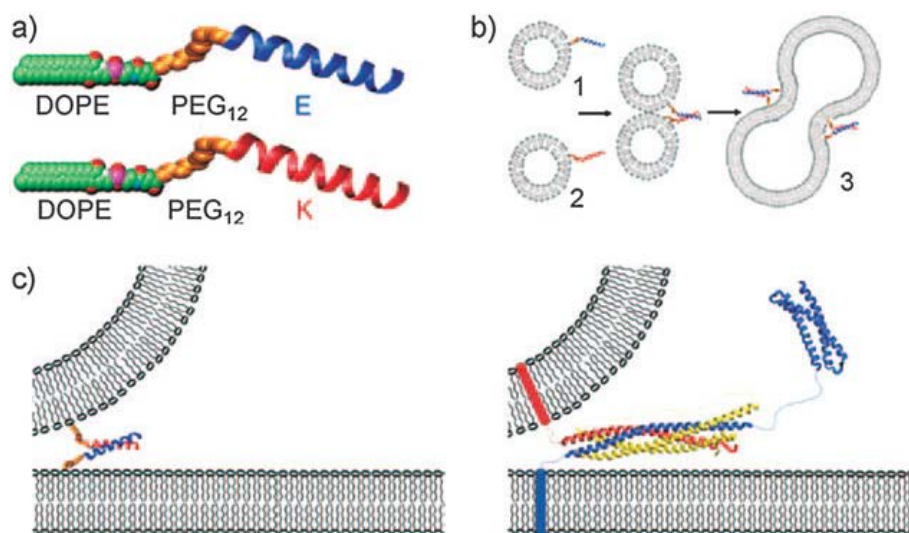
Figure 9. *(a) Space filling models of LPE and LPK. (b) Liposomes are decorated with LPE or LPK and upon mixing, coiled coil formation occurs. This brings the liposomes into close proximity, and induces fusion. (c) Comparison of the minimal model (left) with the natural SNARE-protein-based model (right). Adapted from ref. 30.*

Two lipidated peptides were synthesized, LPE and LPK. The peptides E and K form an α-helical heterodimeric coiled coil when they come into close contact in aqueous solution. To the N-terminus of both of these peptides a flexible spacer was attached, which was then conjugated with a hydrophobic anchor. Two batches of liposomes were prepared, either decorated with LPE or LPK. Upon mixing it was shown that the molecular recognition between the peptides E and K led to aggregation followed by fusion of the liposomes. The inner as well as the outer lipid leaflets were mixed, and the contents of the liposomes were mixed without any leakage. In this multicomponent system several interactions are combined. The self-assembly of the lipids into liposomes is driven by hydrophobic interactions, which also drives the anchoring of the hydrophobic tail of the lipopeptides into the bilayer. Hydrogen bonding enables the peptide residues to be in an α-helical secondary structure. The formation of coiled coils is mainly governed by hydrophobic interactions between amino acids in particular positions of the peptide helices.

4. Applications

Applications of PAs as discussed in this chapter are of interest in a wide range of research fields, ranging from catalysis to regenerative medicine.[1] PAs can be used to direct the formation of inorganic crystals through biomineralization.[31] The PA

assemblies act as a template from which spatially controlled assemblies of inorganic nanoparticles can be formed. Recent contributions have seen controlled growth of calcite,[13,32] hydroxyapatite,[33] cadmiumsulfide,[34] and gold[35] nanoparticles. Designing efficient new drug delivery systems is one of the focus points in the peptide amphiphile community. Most current drug molecules are rapidly degraded in the body, they are not targeted to a specific cell type, and there is no control over the local concentration. PAs can be useful for the targeting of a specific receptor.[36] Carriers consisting solely of PA molecules can solubilize hydrophobic drugs in their lipid-tail core. Furthermore, it was shown that these features can be combined by including a target-specific amino acid sequence, intended to direct the uptake of the drugs by a specific cell type.[37] However, the delivery of intact micelles is troubled by the dynamic nature of this supramolecular structure. A recent investigation shows the uptake of monomers of an acylated pro-apoptotic peptide instead of complete micelles, which is due to the weak non-covalent interactions which bind the Pas in the micelles.[38] Peptide amphiphiles containing the Arg-Gly-Asp (RGD) epitope have been found to adhere to cells, promote cell invasion, and inhibit metastasis.[39] However, drugs based on RGD containing PAs are often degraded rapidly and excreted from the body. By localizing RGD PAs at the surface of liposomes, enhanced structural stability was observed, resulting in longer half-lives and enhancing their antimetastatic activity.[40] Higher binding affinity to cells was observed by restraining the RGD sequence to a loop conformation, which was accomplished by alkylation of the peptide at both the N and C termini.[41] Another way to induce a looped conformation is by the synthesis of cyclic RGD containing peptides.[42, 43] Antimicrobial[2] or antiseptic agents[44] based on PAs have been developed. In both cases, the conjugation of the peptide to a hydrophobic moiety increased the activity, by inducing a well-defined secondary structure of the peptide at the membrane of the targeted cell. PAs are also used as an imaging tool. For this a peptide amphiphile was designed with a chelating agent to coordinate a gadolinium ion, a bioactive segment to target a specific cell receptor, and a hydrophobic tail to induce self-assembly.[45] In this way the position of the PA in the body could be easily determined by magnetic resonance imaging. Synthetic three-dimensional matrices that can stimulate and direct cell proliferation and differentiation are vital in the field of regenerative medicine. PA nanofibers were able to bind heparin and subsequently form a gel in which growth factors for angiogenesis were added.[46] This system was found to substantially increase

the formation of new blood vessels from existing ones for the treatment of ischemic heart disease. The final example demonstrates the enormous potential of functional PA assemblies in regenerative medicine. Network consisting of PA nanofibers was shown to function as a scaffold, directing the differentiation of neural progenitor cells largely into neurons, while simultaneously quenching astrocyte differentiation.[47] This system was tested in vivo in mice that had been paralyzed due to spinal cord injuries. The PA was injected into the damaged region of the spinal cord, after which gelation occurred. The bioactive gel promoted the growth of neurons, which reconnected the severed spinal cord, and led to regained movement in the paralyzed mice.[48]

5. Conclusions and future prospects

In this chapter the intra- and intermolecular interactions of PAs, and how these influence the self-assembly processes of PA nanostructures were discussed. The hydrophobic block of the PA induces aggregation, which in turn increases the local peptide concentration, inducing and stabilizing the secondary structure of the peptide. However, a second structural block is sometimes needed to restrict a specific peptide segment to the desired three-dimensional orientation. It was observed that when the hydrophobic interaction between the tails is too large, the peptide cannot form a well-defined secondary structure. The secondary structure of the peptide has been shown to influence the morphology of the aggregates. While ordinary single tail surfactants tend to form spherical micelles, PAs often form cylindrical micelles. Furthermore, once the aggregate is formed, a transition in the secondary structure of the peptide can sometimes take place, either triggered externally (by variations in pH or ionic strength) or spontaneously, which can significantly affect the morphology of the aggregate. Also, molecular recognition between peptides or between peptides and DNA can lead to significant structural changes in the assemblies. An increasing understanding of the contributing forces within PA nanostructures is allowing scientists to achieve ever more precise control over the structural and functional properties of these assemblies.

References
1. S. Cavalli, F. Albericio and A. Kros, *Chem. Soc. Rev.*, 2010, **39**, 241-263.
2. Y. C. Yu, M. Tirrell and G. B. Fields, *J. Am. Chem. Soc.*, 1998, **120**, 9979-9987.
3. A. F. Chu-Kung, K. N. Bozzelli, N. A. Lockwood, J. R. Haseman, K. H. Mayo and M. V. Tirrell, *Bioconjugate Chem.*, 2004, **15**, 530-535.
4. D. Lowik, J. G. Linhardt, P. Adams and J. C. M. van Hest, *Org. Biomol. Chem.*, 2003, **1**, 1827-1829.
5. M. D. Pierschbacher and E. Ruoslahti, *J. Biol. Chem.*, 1987, **262**, 17294-17298.
6. C. F. Li, J. B. McCarthy, L. T. Furcht and G. B. Fields, *Biochemistry*, 1997, **36**, 15404-15410.
7. N. B. Malkar, J. L. Lauer-Fields, D. Juska and G. B. Fields, *Biomacromolecules*, 2003, **4**, 518-528.
8. I. Kuzmenko, H. Rapaport, K. Kjaer, J. Als-Nielsen, I. Weissbuch, M. Lahav and L. Leiserowitz, *Chem. Rev.*, 2001, **101**, 1659-1696.
9. R. Matmour, I. De Cat, S. J. George, W. Adriaens, P. Leclere, P. H. H. Bomans, N. Sommerdijk, J. C. Gielen, P. C. M. Christianen, J. T. Heldens, J. C. M. van Hest, D. Lowik, S. De Feyter, E. W. Meijer and A. Schenning, *J. Am. Chem. Soc.*, 2008, **130**, 14576-14583.
10. H. Rapaport, K. Kjaer, T. R. Jensen, L. Leiserowitz and D. A. Tirrell, *J. Am. Chem. Soc.*, 2000, **122**, 12523-12529.
11. S. Cavalli, J. W. Handgraaf, E. E. Tellers, D. C. Popescu, M. Overhand, K. Kjaer, V. Vaiser, N. Sommerdijk, H. Rapaport and A. Kros, *J. Am. Chem. Soc.*, 2006, **128**, 13959-13966.
12. S. Cavalli, D. C. Popescu, E. E. Tellers, M. R. J. Vos, B. P. Pichon, M. Overhand, H. Rapaport, N. Sommerdijk and A. Kros, *Angew. Chem.-Int. Edit.*, 2006, **45**, 739-744.
13. J. T. Meijer, M. Henckens, I. J. Minten, D. Lowik and J. C. M. van Hest, *Soft Matter*, 2007, **3**, 1135-1137.
14. G. W. M. Vandermeulen, C. Tziatzios, R. Duncan and H. A. Klok, *Macromolecules*, 2005, **38**, 761-769.
15. S. E. Paramonov, H. W. Jun and J. D. Hartgerink, *Biomacromolecules*, 2006, **7**, 24-26.
16. H. A. Behanna, J. Donners, A. C. Gordon and S. I. Stupp, *J. Am. Chem. Soc.*, 2005, **127**, 1193-1200.
17. L. Ayres, P. Hans, J. Adams, D. Lowik and J. C. M. van Hest, *J. Polym. Sci. Pol. Chem.*, 2005, **43**, 6355-6366.
18. J. M. Smeenk, M. B. J. Otten, J. Thies, D. A. Tirrell, H. G. Stunnenberg and J. C. M. van Hest, *Angew. Chem.-Int. Edit.*, 2005, **44**, 1968-1971.
19. R. C. Elgersma, T. Meijneke, R. de Jong, A. J. Brouwer, G. Posthuma, D. T. S. Rijkers and R. M. J. Liskamp, *Org. Biomol. Chem.*, 2006, **4**, 3587-3597.
20. F. Boato, R. M. Thomas, A. Ghasparian, A. Freund-Renard, K. Moehle and J. A. Robinson, *Angew. Chem.-Int. Edit.*, 2007, **46**, 9015-9018.
21. S. E. Paramonov, H. W. Jun and J. D. Hartgerink, *J. Am. Chem. Soc.*, 2006, **128**, 7291-7298.
22. T. Shimada, S. Lee, F. S. Bates, A. Hotta and M. Tirrell, *J. Phys. Chem. B*, 2009, **113**, 13711-13714.
23. T. Muraoka, C. Y. Koh, H. G. Cui and S. I. Stupp, *Angew. Chem.-Int. Edit.*, 2009, **48**, 5946-5949.

24. H. Cui, T. Muraoka, A. G. Cheetham and S. I. Stupp, *Nano Lett.*, 2009, **9**, 945-951.
25. F. Versluis, I. Tomatsu, S. Kehr, C. Fregonese, A. Tepper, M. C. A. Stuart, B. J. Ravoo, R. I. Koning and A. Kros, *J. Am. Chem. Soc.*, 2009, **131**, 13186-13187.
26. D. N. Woolfson, *Fibrous Proteins: Coiled-Coils, Collagen and Elastomers*, 2005, **70**, 79-87.
27. H. R. Marsden, A. V. Korobko, E. N. M. van Leeuwen, E. M. Pouget, S. J. Veen, N. Sommerdijk and A. Kros, *J. Am. Chem. Soc.*, 2008, **130**, 9386-9393.
28. R. Bitton, J. Schmidt, M. Biesalski, R. Tu, M. Tirrell and H. Bianco-Peled, *Langmuir*, 2005, **21**, 11888-11895.
29. Y. A. Chen and R. H. Scheller, *Nat. Rev. Mol. Cell Biol.*, 2001, **2**, 98-106.
30. H. R. Marsden, N. A. Elbers, P. H. H. Bomans, N. Sommerdijk and A. Kros, *Angew. Chem.-Int. Edit.*, 2009, **48**, 2330-2333.
31. A. Dey, G. de With and N. Sommerdijk, *Chem. Soc. Rev.*, 2010, **39**, 397-409.
32. D. C. Popescu, M. M. J. Smulders, B. P. Pichon, N. Chebotareva, S. Y. Kwak, O. L. J. van Asselen, R. P. Sijbesma, E. DiMasi and N. Sommerdijk, *J. Am. Chem. Soc.*, 2007, **129**, 14058-14067.
33. J. D. Hartgerink, E. Beniash and S. I. Stupp, *Science*, 2001, **294**, 1684-1688.
34. H. Bekele, J. H. Fendler and J. W. Kelly, *J. Am. Chem. Soc.*, 1999, **121**, 7266-7267.
35. L. S. Li and S. I. Stupp, *Angew. Chem.-Int. Edit.*, 2005, **44**, 1833-1836.
36. M. J. Webber, J. Tongers, M. A. Renault, J. G. Roncalli, D. W. Losordo and S. I. Stupp, *Acta Biomater.*, 2010, **6**, 3-11.
37. S. Keller, I. Sauer, H. Strauss, K. Gast, M. Dathe and M. Bienert, *Angew. Chem.-Int. Edit.*, 2005, **44**, 5252-5255.
38. D. Missirlis, H. Khant and M. Tirrell, *Biochemistry*, 2009, **48**, 3304-3314.
39. N. Oku, C. Koike, Y. Tokudome, S. Okada, N. Nishikawa, H. Tsukada, M. Kiso, A. Hasegawa, H. Fujii, J. Murata and I. Saiki, *Adv. Drug Deliv. Rev.*, 1997, **24**, 215-223.
40. T. Asai and N. Oku, in *Liposomes, Pt E*, ed. N. Duzgunes, 2005, vol. 391, pp. 163-192.
41. T. Pakalns, K. L. Haverstick, G. B. Fields, J. B. McCarthy, D. L. Mooradian and M. Tirrell, *Biomaterials*, 1999, **20**, 2265-2279.
42. V. Marchi-Artzner, M. J. Brienne, T. Gulik-Krzywicki, J. C. Dedieu and J. M. Lehn, *Chem.-Eur. J.*, 2004, **10**, 2342-2350.
43. V. Marchi-Artzner, B. Lorz, C. Gosse, L. Jullien, R. Merkel, H. Kessler and E. Sackmann, *Langmuir*, 2003, **19**, 835-841.
44. C. Mas-Moruno, L. Cascales, L. J. Cruz, P. Mora, E. Perez-Paya and F. Albericio, *ChemMedChem*, 2008, **3**, 1748-1755.
45. A. Morisco, A. Accardo, E. Gianolio, D. Tesauro, E. Benedetti and G. Morelli, *J. Pept. Sci.*, 2009, **15**, 242-250.
46. K. Rajangam, H. A. Behanna, M. J. Hui, X. Q. Han, J. F. Hulvat, J. W. Lomasney and S. I. Stupp, *Nano Lett.*, 2006, **6**, 2086-2090.
47. G. A. Silva, C. Czeisler, K. L. Niece, E. Beniash, D. A. Harrington, J. A. Kessler and S. I. Stupp, *Science*, 2004, **303**, 1352-1355.
48. V. M. Tysseling-Mattiace, V. Sahni, K. L. Niece, D. Birch, C. Czeisler, M. G. Fehlings, S. I. Stupp and J. A. Kessler, *J. Neurosci.*, 2008, **28**, 3814-3823.